Mass transfer correlations for nonaqueous phase liquid dissolution from regions with high initial saturations

Indumathi M. Nambi[1] and Susan E. Powers

Department of Civil and Environmental Engineering, Clarkson University, Potsdam, New York, USA

Received 9 May 2001; revised 6 June 2002; accepted 6 June 2002; published 12 February 2003.

[1] The application of existing correlations for nonaqueous phase liquid (NAPL) dissolution, which were developed in small, one-dimensional columns, to larger-scale, heterogeneous or multidimensional systems has shown the predicted dissolution behavior depends greatly on the correlation used. Variation among existing correlations is due to the system scale, NAPL-water interfacial area, and the nature of mass transfer or hydrodynamic mechanisms that are lumped in the correlation. In this paper, new mass transfer correlation is developed using NAPL dissolution data from a small 2-D experimental cell that contained a well-characterized heterogeneous distribution of grain sizes. The new correlation can be used for quantifying NAPL dissolution rates over a wide range of NAPL saturations and aqueous phase velocities within the NAPL source zone. When incorporated in a finite difference transport model, the correlation provides reasonably good predictions for systems with initially high NAPL saturations that are then reduced through the dissolution process. It is shown that NAPL dissolution is slower in this case due to the larger amorphous blobs that result from preferential flow and dissolution pathways. These large blobs have significantly less surface area in comparison with small discrete blobs that result from capillary entrapment. In comparison with other published dissolution correlations, the slower mass transfer rate is characterized with a significantly higher exponent on the NAPL saturation term. *INDEX TERMS:* 1803 Hydrology: Anthropogenic effects; 1832 Hydrology: Groundwater transport; *KEYWORDS:* NAPL, dissolution, heterogeneous media, Sherwood number, mass transfer correlation

Citation: Nambi, I. M., and S. E. Powers, Mass transfer correlations for nonaqueous phase liquid dissolution from regions with high initial saturations, *Water Resour. Res.*, *39*(2), 1030, doi:10.1029/2001WR000667, 2003.

1. Introduction

[2] Subsurface heterogeneity affects NAPL migration and dissolution rates, thereby affecting levels of groundwater contamination and the effectiveness of remediation strategies. Heterogeneities in the pore size distribution over a wide range of scales can be important [*Chatzis et al.*, 1983; *Kueper et al.*, 1989; *Wilson et al.*, 1990; *Illangasekare et al.*, 1995; *Powers et al.*, 1998]. Even the fine bedding planes of the Borden aquifer cause a very wide distribution of NAPL saturations (0.01–0.38) over a scale of several centimeters [*Kueper et al.*, 1993]. This heterogeneity in the NAPL saturation is coupled with spatial and temporal variation in aqueous phase velocities as NAPL saturations decrease due to dissolution. These variations cause significant changes in the flow patterns with bypassing of water around regions of low effective permeability and preferential flow through regions of high permeability [*Powers et al.*, 1998; *Nambi and Powers*, 2000; *Saba and Illangasekare*, 2000].

[3] The impact of heterogeneity on NAPL dissolution can be noted by observing differences in the results of dissolution experiments in heterogeneous systems when compared with those from homogeneous columns. Effluent concentrations from homogeneous columns generally are close to their equilibrium concentrations for an initial period; followed by a steady decline in concentrations as the NAPL saturation is reduced [*Imhoff et al.*, 1994; *Powers et al.*, 1994]. In heterogeneous systems comprised of a NAPL contaminated region surrounded by clean media, variable flow rates and mass transfer rate limitations create concentration profiles with distinct periods of increasing and then decreasing concentrations [*Geller and Hunt*, 1993; *Powers et al.*, 1998; *Nambi and Powers*, 2000]. Longer clean up times have also been observed in these systems. *Powers et al.* [1998] attributed the initial phase to higher mass fluxes as the relative permeability of the NAPL source zone increases. Later, decreases in the downstream concentrations are correlated to decreases in the NAPL saturation below a critical value for which mass transfer in the NAPL source zone (several centimeters in this case) appears to be a rate limited process.

[4] A stochastic approach has been used in several recent efforts to mathematically model NAPL dissolution in heterogeneous systems [*Mayer and Miller*, 1996; *Berglund*, 1997; *Unger et al.*, 1998; *Zhu and Sykes*, 2000; *Dekker and Abriola*, 2000]. Correlations for mass transfer coefficients, which were developed for homogeneous systems, were applied to define mass transfer rates. Aqueous phase velocities and the choice of mass transfer correlations were found

[1]Now at the Department of Civil and Environmental Engineering, University of Illinois, Urbana, Illinois, USA.

Copyright 2003 by the American Geophysical Union.
0043-1397/03/2001WR000667

to have more pronounced effects in heterogeneous media than homogeneous media [*Mayer and Miller*, 1996]. *Unger et al.* [1998] concluded that the choice of dissolution rate correlation has greater influence on DNAPL dissolution in heterogeneous systems than the uncertainty in DNAPL distribution or spatial heterogeneity. These studies indicate the inadequacy of the existing correlations and emphasized the need for better mass transfer correlations. Thus, the overall objective of this research was to generate a new mass transfer correlation that incorporates a broader range of mechanisms that affect NAPL dissolution in heterogeneous systems.

2. Background

[5] In the past decade of study, two basic approaches have been used to estimate NAPL dissolution rates. A local equilibrium approach (LEA) allows the rate of mass transfer to be estimated based on an equilibrium partitioning relationship [e.g., *Abriola*, 1989]. An alternative approach, which acknowledges that equilibrium is not achieved at all scales, estimates the dissolution rate with a linear driving force model [*Cussler*, 1997]:

$$r_i = k_i a_o \left(C_i^* - C_i \right) \tag{1}$$

where r_i is the mass transfer rate per unit volume [M L^{-3} t^{-1}]; k_i is the mass transfer coefficient [L t^{-1}]; a_o is the specific surface area between the two phases [L^{-1}]; and C_i is the aqueous phase concentration [M L^{-3}] of species i with superscript * indicating the concentration that would be in equilibrium with the bulk NAPL. *Hunt et al.* [1988] first applied this model to estimate NAPL dissolution rates.

[6] Both of these approaches are fraught with uncertainties. The LEA requires definition of the ''local'' scale over which this assumption is applicable and quantification of the volumes of the two fluids that are equilibrated. The linear driving force model requires an estimate of k_i and a_o or the mass transfer rate coefficient ($\hat{k} = k_i a_o$), which lumps limitations due to the surface area between the phases with other mechanisms that affect mass transfer rates. Depending on the scale and dimensionality of measurement and the various processes that affect the net dissolution rate, mass transfer coefficients developed from experimental data are typically highly system dependent.

[7] Correlations for mass transfer rate coefficients have been published in numerous studies for the dissolution of residual NAPL blobs [*Miller et al.*, 1990; *Geller and Hunt*, 1993; *Powers et al.*, 1992, 1994; *Imhoff et al.*, 1994; *Dillard and Blunt*, 2000; *Zhou et al.*, 2000] and NAPL pools [*Kim and Chrysikopoulos*, 1999; *Chrysikopoulos and Kim*, 2000]. Almost all of these were developed for small-scale systems with uniform NAPL saturations and flow fields. Modeling studies have shown that there are huge differences in the predicted clean up time in large-scale [*Zhu and Sykes*, 2000] or heterogeneous [*Mayer and Miller*, 1996] systems when different mass transfer rate coefficient correlations are used.

[8] The use of mass transfer coefficients to describe interphase mass transfer phenomena is based on conceptual models of fluid flow and diffusion processes near the interface. The classic film theory, for example, identifies a thin film of fluid near the interface that is not mixed with the bulk fluid phase and therefore creates a resistance to mass transfer [e.g., *Cussler*, 1997]. The scale of this film is on the order of a few to several water molecules. Table 1 identifies some of the many additional mechanisms that limit the net mass transfer rate during NAPL dissolution processes. Some of the pore scale mechanisms are described well with the classical theory of mass transfer, although other mechanisms that affect dissolution in larger scale systems are not. Thus, the practical application of mass transfer coefficients in complex subsurface systems often results in the incorporation of mechanisms that are not consistent with the classical definition of these coefficients. Depending on the experimental system used to generate data, mechanisms included in the mass transfer correlation can vary substantially.

Table 1. Some Mechanisms That Limit the Dissolution of NAPL Entrapped in Porous Media

Scale and Mechanism	Citations
Pore scale	
Pore diffusion, corner diffusion, and mixing within and between pores	*Jia et al.* [1999], *Zhou et al.* [2000], *Dillard and Blunt* [2000]
Bypassing of water around pores with NAPL	*Zhou et al.* [2000]
Laboratory scale	
Limited contact time between phases at high aqueous phase flow rates	*Miller et al.* [1990], *Powers et al.* [1992]
Limited NAPL surface area accessible to flow	*Lamarche* [1991], *Powers et al.* [1994]
Bypassing of water around pores with NAPL	*Soerens et al.* [1998]
Dissolution fingering	*Imhoff et al.* [1996]
Bypassing of aqueous phase around regions with NAPL due to reduced effective permeability (2-D systems)	*Powers et al.* [1998], *Saba and Illangasekare* [2000]
Field scale	
Bypassing of aqueous phase around regions with NAPL due to reduced effective permeability	*Frind et al.* [1999]

[9] A fundamental problem with incorporating presently available mass transfer correlations into models for large scale or heterogeneous systems is the failure of these correlations to capture the appropriate physical phenomena that dominates NAPL dissolution in the modeled systems. The *Powers et al.* [1994] and *Imhoff et al.* [1994] correlations have been used most extensively. The Powers correlation was based on uniform residual saturations in a range of homogeneous media that resulted from a series of immiscible fluid displacement steps. Their incorporation of a ratio of the volumetric NAPL saturation at any point in time to the initial volumetric saturation ($\theta_{in}/\theta_{in}^{o}$) greatly restricts the applicability of their correlation to only other systems with similar initial saturations [*Zhu and Sykes*, 2000]. The Imhoff correlation was based on data from a column that was long enough to illustrate the significant impact of dissolution fingering on the net mass transfer rate. Although the inclusion of this phenomenon in the correlation makes it better suited for larger scale application, the 7-cm experimental column is still substantially different from field-scale systems.

[10] Two approaches can be used to incorporate multiple mechanisms that effectively reduce the net mass transfer flux during NAPL dissolution. Although many mechanisms, such as dissolution fingering, are associated with a process other than diffusion of the solute at the interface, the

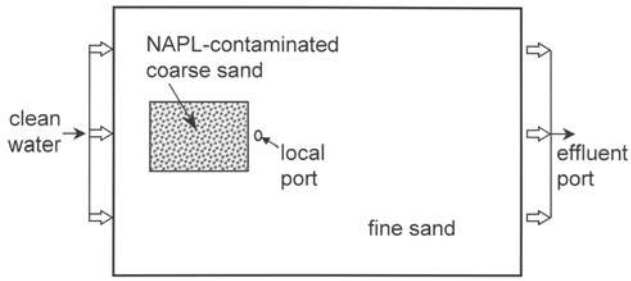

Figure 1. Front view of the two-dimensional cell experimental cell used by *Nambi and Powers* [2000]. Dimensions of the cell are 17.8 cm × 12 cm × 2.9 cm. The size and number of coarse sand lenses, initial NAPL saturation within the coarse sand lens, and ratio of permeability in the fine to coarse sand were varied between experiments. Mechanisms within the coarse sand lens that affect NAPL dissolution rates were the focus of this first paper.

net effect of these processes can be lumped into a correlation for the mass transfer rate coefficient [e.g., *Powers et al.*, 1994; *Imhoff et al.*, 1994]. Alternatively, if the hydrodynamics of the porous medium can be characterized at an appropriate scale, the net mass transfer rate can be described with an analysis of the system hydrodynamics at that scale along with an equilibrium assumption or suitable mass transfer coefficient [*Sorens et al.*, 1998; *Powers et al.*, 1998; *Frind et al.*, 1999; *Zhou et al.*, 2000; *Saba and Illangasekare*, 2000]. Either of these approaches should be valid for modeling NAPL dissolution in heterogeneous systems. Adequate definition of the hydrodynamics at an appropriate scale has been accomplished for well-characterized systems at pore [*Zhou et al.*, 2000; *Knutson et al.*, 2001], laboratory [*Powers et al.*, 1998; *Saba and Illangasekare*, 2000; *Brusseau et al.*, 2002], and field scales [*Frind et al.*, 1999].

[11] The objective of this research was to develop a method for estimating dissolution rates for NAPL initially entrapped at high saturations, such as could be found in a coarse lens of a heterogeneous medium. The work presented here analyzes NAPL dissolution data presented by *Nambi and Powers* [2000], which incorporate rate-limiting mechanisms important in systems with complex NAPL distributions.

3. Experimental Details

[12] Experimental data from a simplified heterogeneous system comprised of a well-defined coarse sand lens surrounded by a finer medium (Figure 1) were used as the basis for the mass transfer coefficient correlations developed in this paper. The overall dimensions of this cell were 17.8-cm long by 12-cm high by 2.9-cm wide. *Nambi and Powers* [2000] describe details of the experimental procedure and results. An overview of the methods is included here.

[13] A known amount of NAPL (o- toluidine) was injected directly into the coarse lens where it was retained by capillary forces. The initial NAPL saturation was estimated from the volume injected. Changes in the NAPL saturation over the course of an experiment were estimated by mass balance. Solute concentrations in the aqueous phase that passed through the coarse lens, were measured by sampling at a local port located immediately downstream of the NAPL source zone. The fraction of the flow passing through the coarse sand lens that was captured at this sampling point was initially very large, but decreased over time as the velocity of water increased. Additional aqueous phase samples were collected at the outlet of the system to provide information for a system mass balance. Samples were collected until the NAPL concentrations in the aqueous phase were reduced to below analytical detection limits. This represented approximately a three order of magnitude reduction in concentration. Several dissolution experiments were conducted with a range of experimental conditions: variables included initial NAPL saturation (0.3 to 0.8), grain size of sands (0.036 to 0.15 cm), width of the coarse lens (1.5 to 3 cm) and number of coarse lenses (1 to 2). All experiments showed similar trends in the concentrations measured at the local port [*Nambi and Powers*, 2000].

[14] A typical concentration history at the local port is shown in Figure 2. The concentrations remained at a constant value, at or near the equilibrium concentration for the first phase of the experiment, after which a steep drop in the concentration was observed for several pore volumes. A long tail of very low concentrations was observed at the end of many of the experiments. During the initial phase of the experiment (PV < ~20; Figure 2), the establishment of an equilibrium condition at the local scale of this experimental system resulted from several mass transfer and hydrodynamic mechanisms operating at different scales [*Nambi and Powers*, 2000]. Concentrations close to the equilibrium value prevented the quantification of mass transfer coefficients for this period. Based on visual observation, NAPL dissolved from the coarse sand lens by the end of the period of interest (~35 PV). The subsequent long tailing period, which is most likely the result of desorption and diffusion of solutes from the very fine media at the top of the experimental cell, was also not considered in the analysis because these concentrations were greatly affected by mechanisms other than those limiting the NAPL

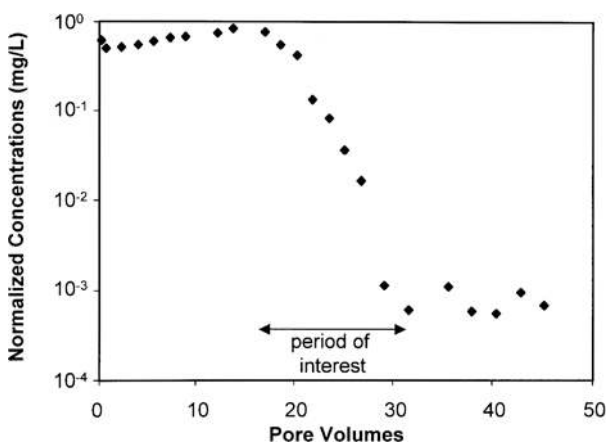

Figure 2. A typical profile of the normalized (C/C*) o-toluidine concentrations measured at the local port. These are the results of a dissolution experiment with a single coarse lens of dimensions 5 cm × 3 cm (10–18 mesh size sand) embedded in finer medium (30–40 mesh size sand). The arrows indicate the times when mass transfer is rate limited within the NAPL source zone.

source dissolution. Thus, the work presented here to quantify mass transfer coefficients for a well-characterized NAPL source zone over a wide range of initial NAPL saturations focuses on the middle portion of these curves. Development of mass transfer coefficient correlations in this system requires that the NAPL saturations and aqueous phase velocity distribution also be quantified within the source zone.

4. Research Methodology

[15] A multistep methodology was used to develop a mass transfer correlation for the NAPL source zone; starting from data reduction and processing followed by a regression analysis. The correlation was then subjected to a sensitivity analysis in order to assess the influence of the assumed parameters on the overall model. Finally the validity of the correlation was verified by comparing independent data sets to predictions made by a finite difference solute transport model that incorporated the correlation.

4.1. Data Reduction

[16] In the experimental system considered here, it has been established that equilibrium conditions govern the local mass transfer process at NAPL saturations greater than approximately 0.3 ± 0.05 [*Nambi and Powers*, 2000]. The net dissolution process within the NAPL source zone considered at the scale of these experiments was measurably rate limited at lower saturations. Hence only the partial concentration data for rate limited conditions were included in the correlation (Figure 2).

[17] Concentrations measured at the port immediately downgradient of the NAPL source were used to calculate the mass transfer coefficients for the source zone for each point in time. The mass transfer rate coefficient was calculated as [*Powers et al.*, 1992]:

$$\hat{k} = -\frac{q}{L}\ln\left(\frac{C^* - C}{C^*}\right) \tag{2}$$

where q is the Darcy velocity, and L is the length of the NAPL source zone. Subscripts indicating the species of interest are dropped here because a single-component NAPL was employed.

[18] Application of equation (2) over a differential element in time to experimental data required assumptions that the aqueous phase flow vectors were essentially one dimensional through the source zone and that losses due to transverse dispersion were negligible. Modflow simulations by *Powers et al.* [1998] and *Nambi and Powers* [2000] illustrate that assumptions regarding one-dimensional flow and minimal lateral dispersion during the period of interest are justified. Dispersion was found to contribute substantially to mass loss at the early stages of the experiments when the very low effective permeability of the coarse sand caused greater flow around this region. This stage corresponds to the local equilibrium stage in the concentration profile (Figure 2; 0–20 PV). At later stages, when the flow through the coarse lens was higher, lateral dispersion became negligible when compared to the longitudinal advection term. Since the early time data was not used in this analysis, the assumption that lateral dispersion is negligible is valid.

[19] The Darcy velocity, which is required in equation (2), was calculated by averaging the flow through the coarse lens over the cross-sectional area of the lens. The flow through the coarse lens, Q_c, was estimated using Darcy's law and flow balance equations. It was assumed that water flow lines through the fine and coarse sands remain parallel, allowing the piezometric head gradients through both of the sands to be equated [*Nambi and Powers*, 2000]. This approach neglects the small regions of diverging and converging flow lines at either end of the source zone. The overall approach and equations that were used for estimating Q_c were outlined by *Powers et al.* [1998].

[20] Application of Darcy's equation required estimates of the intrinsic permeability of the fine sand and effective permeability of the coarse sand. The intrinsic permeabilities of the sands were measured by constant head permeability experiments [*American Society for Testing and Materials* (*ASTM*), 1993]. The effective permeability of the coarse sand was calculated using Corey's relationship for relative permeability as a function of water saturation [*Corey*, 1954]:

$$k_r = S_e^4 = \left(\frac{S_w - S_{r_w}}{1 - S_{r_w}}\right)^4 \tag{3}$$

where S_e is the effective aqueous phase saturation, S_w is the aqueous phase saturation ($S_w = 1 - S_n$); and S_{rw} is the irreducible water saturation which generally lies in the range 0.05–0.15 [*Wilson et al.*, 1990]. *Powers et al.* [1998] showed that use of the Corey equation to estimate the distribution of flow in similar types of experiments provided the best estimates for the early time data that could be described by a local equilibrium assumption. A sensitivity analysis, which is presented later in this paper, evaluates the adequacy of this assumption by comparing correlations developed with equation (3) to those estimated with Wyllie's equation [*Wyllie*, 1962]. This means of estimating relative permeabilities employs an exponent of three rather than four in the Corey equation (equation (3)).

[21] NAPL saturations were estimated by employing a mass balance approach. *Powers et al.* [1998] illustrated that it is reasonable to average the NAPL saturation over the entire volume of the coarse lens at any point in a dissolution experiment. They verified the accuracy of this approach by performing direct quantification using styrene polymerization technique and found that the NAPL saturations estimated by mass balance approach varied only by ±2%. The initial NAPL saturations were calculated from the known volume of NAPL injected into the coarse lens. Average saturations at later times were established based on the premise that mass dissolved from the NAPL over any time period equals the mass of solute in the effluent of the experimental cell over that period. A numerical integration of the effluent concentration as a function of pore volume throughput was employed in these calculations.

[22] As a result of the above calculations, the experimentally measured data from *Nambi and Powers* [2000] were reduced to a matrix of parameters. The mass transfer rate coefficients (equation (1)) represent the dependent variable. Potential independent variables affecting mass transfer rates included NAPL saturation, velocity of water through the coarse lens, dimensions of the sand lens, sand grain size and intrinsic permeability. A total of 90 data sets from 9 experiments were used in the development of the correla-

tion. Results from two other experiments were reserved for verification of the correlation. These two experiments were chosen such that their initial NAPL saturations fell at the extremes of the range of initial NAPL saturations used in the other experiments.

4.2. Regression Analysis

[23] The Gilland-Sherwood type relationship, which has been extensively used for mass transfer coefficient correlations, was considered appropriate here [e.g., *Cussler*, 1997]. As with most other NAPL dissolution correlations, the traditional Sherwood number was modified to incorporate the mass transfer rate coefficient that lumps the specific surface area with the mass transfer coefficient. The modified Sherwood number is defined as:

$$Sh' = \frac{\hat{k} l_c^2}{D_l} \tag{4}$$

where l_c is a characteristic length and D_l is the diffusion coefficient for the organic solute in water. The diffusion coefficient for o-toluidine was estimated to be 7.5×10^{-6} cm^2/s using the Wilke and Chang empirical equation [*Cussler*, 1997].

[24] Identifying the appropriate independent variables included in Sherwood number correlation is a critical step in the overall development of a mass transfer correlation. A suite of all possible independent variables must be identified initially, with the most significant ones determined through the regression analysis. A careful analysis of the processes influencing mass transfer coupled with the knowledge derived from the work of other researchers enabled identification of the variables that are potentially important. Variables incorporated into other NAPL dissolution correlations were considered here with the exception of the Schmidt number [*Miller et al.*, 1990] and the length of the NAPL zone [*Imhoff et al.*, 1994] because neither of these varied in the experiments analyzed here.

[25] The importance of NAPL saturation and aqueous phase velocities in determining mass transfer rates has been well established from previous studies in homogeneous systems with low NAPL saturations [*Miller et al.*, 1990; *Imhoff et al.*, 1994; *Powers et al.*, 1994]. Other parameters that could potentially influence the interfacial area available for mass transfer were identified as porous medium grain size [*Powers et al.*, 1992] and size of the contaminated region as a whole [*Nambi and Powers*, 2000]. The interstitial velocity, which is the Darcy velocity divided by the effective porosity [$\phi_{eff} = \phi\ (1 - S_n)$] and a Reynolds number that is based on the interstitial velocity, Re′, are used throughout in the following discussions.

[26] Both the relative size of the sand grains used in these experiments and the absolute grain size could affect mass transfer rates. The median grain size of the coarse sand normalized by the diameter of a medium sand as defined by USDA ($\delta = d_{50}/d_M$ where $d_M = 0.05$ cm) was included as one of the parameters. This parameter directly influences the specific surface area of NAPL blobs entrapped in one or a few pore spaces [*Powers et al.*, 1992]. The effective permeability of the coarse lens determined the hydrodynamics of the heterogeneous system and the velocity of water through the contaminated zone. Since relative permeability is not an independent parameter ($k_r = f(S_n, k_c)$), the intrinsic permeability was identified as a potentially significant parameter and was represented in its dimensionless form by the ratio of intrinsic permeabilities of coarse and fine sands ($\kappa = k_c/k_f$).

[27] *Nambi and Powers* [2000] concluded that the external surface area of the NAPL source zone was an important variable affecting the overall mass transfer behavior. To incorporate this variable, the width of the coarse lens was chosen to represent the size of contaminated region since it was varied between experiments. It was included in the correlation as its proportion of the total width of the experimental cell. ($\omega = w_c/W$).

[28] The Gilland Sherwood correlation for the heterogeneous system considered in this study was formulated with the above dimensionless groups as

$$Sh' = \alpha S_n^{\beta_1} \mathrm{Re}'^{\beta_2} \delta^{\beta_3} \omega^{\beta_4} \kappa^{\beta_5} \tag{5}$$

The logarithm was used to transform this equation into a linear form so that linear regression analysis could be employed to determine correlation coefficients (α, β_i). The multiple linear regression tool within the Microsoft Excel software was used to obtain the estimates of the coefficients.

[29] A stepwise regression technique was employed to systematically evaluate optimum combinations of the parameters for the phenomenological model in order to obtain the best fit to the experimental data. The first regression was done with only the first variable, NAPL saturation. The stepwise regression procedure involved the stepwise addition of the other individual parameters. After each addition of a parameter, the new model was assessed for its quality of fit to the data and its adequacy by comparing the coefficient of determination, R^2, among correlations and by performing an F test. R^2 is a percentage measure of the variability in Sherwood number that can be accounted by the variability in the other variables. The F test for assessing the utility of the overall model was employed by checking the null hypothesis, that all $\beta_i = 0$ versus at least one of the $\beta_i \neq 0$ [*Mendenhall and Sincich*, 1994]. The probability value, (p value) or in statistical terms the observed significance level associated with the F statistic, gives a measure of the disagreement of the test statistic with the null hypothesis. A significance level of 0.05, which gives a 95% confidence in deciding whether the null hypothesis can be rejected, was chosen in this analysis.

[30] The statistical significance of each parameter added in a stepwise fashion was also evaluated using the two-sided t test. Based on the results of these analyses the importance of the added value on the overall model performance was evaluated and the parameter was either accepted or rejected. In this test, the null hypothesis, H_0: $\beta_i = 0$ was checked against the alternative hypothesis, H_a: $\beta_i \neq 0$ for every added parameter. Similar to the F- test, if the p value corresponding to the t statistic of the coefficient β_i was less than a chosen significance level (0.05), the null hypothesis was rejected and the parameter associated with that coefficient was considered to be of statistical significance.

5. Results and Discussion

[31] The results of the stepwise regression procedure are presented in Table 2. The high R^2 values (0.92–0.94) and

Table 2. Results of the Stepwise Regression

Correlation	R^2	F statistic (p Value)	t Statistic of the Added Parameter (p Value)
$Sh' = 7.94\ S_n^{1.22}$	0.92	874 (9.81×10^{-43})	29.57 (9.8×10^{-43})
$Sh' = 37.15\ S_n^{1.24}\ Re'^{0.61}$	0.94	548 (1.06×10^{-44})	4.30 (5.75×10^{-5})
$Sh' = 54.95\ S_n^{1.24}\ Re'^{0.55}\ \delta^{0.15}$	0.94	361 (2.63×10^{-43})	0.36 (0.717)
$Sh' = 68.39\ S_n^{1.26}\ Re'^{0.70}\ \kappa^{-0.16}$	0.94	363 (2.21×10^{-43})	−0.70 (0.49)
$Sh' = 18.20\ S_n^{1.25}\ Re'^{0.65}\ \omega^{-0.68}$	0.94	380 (4.43×10^{-44})	−1.95 (0.06)

the very low probability values ($2.2 \times 10^{-42} - 1.42 \times 10^{-45}$) associated with the F statistic of all the models indicate that they all have a high utility value. NAPL saturation was identified as the most important parameter that controls NAPL dissolution for the experimental data considered here. It was observed that almost 92% of the variation in Sherwood numbers was explained by variations in NAPL saturations alone. The p value associated with the t statistic of NAPL saturation is very low providing further evidence of its importance. Based on a p value < 0.05, the Reynolds number was also identified as a statistically significant parameter necessary to quantify mass transfer. The p values associated with the t statistic of the parameters δ, κ, and ω were greater than the chosen value (0.05). This indicates that these parameters are not very significant in describing the overall mechanisms affecting mass transfer in this system.

[32] Based the results of the stepwise regression analysis, the simplest correlation which adequately describes the NAPL dissolution within the coarse sand lens in the two-dimensional system considered here is:

$$Sh' = 37.2\ S_n^{1.24} \mathrm{Re}'^{0.61} \tag{6}$$

Confidence intervals (95%) for each of the coefficients are $17.4 < \alpha < 79.4$; $1.17 < \beta_1 < 1.32$ and $0.32 < \beta_2 < 0.89$. In comparison with the few other papers that have published similar statistical analyses, the confidence intervals for β_1 and β_2 defined above are similar in magnitude, but the interval for α is greater than correlations developed for simpler one-dimensional systems containing a residual saturation of NAPL [*Miller et al.*, 1990; *Powers et al.*, 1994]. Figure 3 presents Sherwood numbers predicted using equation (6) with the Reynolds number and NAPL saturation values used to develop the correlation versus Sherwood numbers calculated directly from experimental data. The quality of fit of the model to the experimental data is very good for all the experiments, with 91% of the measured Sherwood numbers values falling within a factor of 5 of the estimated value.

[33] The model was assessed for statistical validity using an analysis of residuals. Plots of the residual against the independent variables, logarithms of NAPL saturation and Reynolds number did not show any particular pattern (data not shown), which clearly indicated that the model was correctly specified with respect to these independent variables [*Mendenhall and Sincich*, 1994]. A plot of residuals of the new model against the dependent variable, log (Sh') was analyzed to check for unequal variances and presence of outliers. The plot did not show any significant pattern indicating that the variances are equal. There were no points with residuals larger than three times the standard error and, hence, no outliers were identified.

5.1. Comparison With Other Correlations

[34] Table 3 presents a comparison of the mass transfer correlation developed in this work to those developed by other investigators along with the range of Re numbers and NAPL volumetric fractions ($\theta_n = \phi S_n$) for which they are valid. This illustrates that the range of NAPL saturations covered by the correlation developed here is very large and encompasses the ranges of all the existing models. It should be noted here that the Reynolds number (Re') used in the new correlation and Powers correlation represent the seepage velocity whereas the others represent the Darcy velocity.

[35] The new model can be compared with the existing models by examining the coefficients on the Reynolds number and NAPL saturation. The coefficient on the Reynolds number in equation (6) (0.61) is very similar to the one obtained by *Powers et al.* [1994] and within the range of the well-established packed-bed systems (0.56–0.69) published in the chemical engineering literature [e.g., *Treybal*, 1980].

[36] The significant difference in the correlation developed in this work and the others is the coefficient of the NAPL saturation. While almost all the correlations resulted in coefficients less than one (Table 3), the new correlation has a coefficient greater than one. This difference can be directly attributed to the high NAPL saturations used in the experiments. High NAPL saturations are associated with large, continuous or interconnected blobs [*Conrad et al.*,

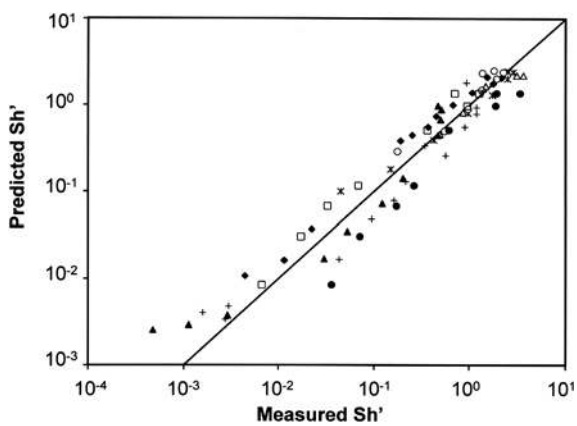

Figure 3. Predicted Sherwood numbers estimated from the new local mass transfer correlation (equation (6)) versus observed Sherwood numbers calculated from experimental concentration data. Each set of symbols represent data from one of seven different experiments.

Table 3. Comparison of Correlations for Modified Sherwood Numbers

Reference	Correlation	Valid Conditions
Miller et al. [1990] (steady state dissolution)	$Sh = 425\ Re^{0.75}\ \theta_n^{0.60}$	$0.016 < \theta_n < 0.07$; $0.0015 < Re < 0.1$
Imhoff et al. [1994][a]	$Sh = 340\ Re^{0.71}\ \theta_n^{0.87}(x/d_p)^{-0.31}$ $Sh = 150\ Re^{0.87}\ \theta_n^{0.79}$	$0 < \theta_n < 0.04$; $0.0012 < Re < 0.021$; $1.4 < x/d_p < 180$
Powers et al. [1994][b]	$Sh = 4.13\ Re'^{0.60}\ \delta^{0.67}\ U_i^{0.37}\ (\theta_n/\theta_n^o)^{\beta}$ where $\beta \sim 0.5-1.0$	$0.0003 < \theta_n < 0.065$; $0.052 < Re' < 0.08$; $1.19 < U_i < 3.33$
This work	$Sh = 37.15\ Re'^{0.61}\ S_n^{1.24}$	$0.01 < S_n < 0.35$; $(0.0048 < \theta_n < 0.168)$; $0.018 < Re < 0.134$

[a]Here x/d_p is the dimensionless distance into the residual saturation zone.
[b]Here θ_n^o is the initial volumetric fraction of NAPL in the system, Re' employs the interstitial velocity.

1992]. Theoretical investigations by *Powers et al.* [1991] showed that the coefficients of NAPL volumetric fraction increased from 0.67 to values closer to 1 when the blob geometry was modified from a small sphere to a long cylinder. *Powers et al.* [1994] fitted the exponent on NAPL volumetric fraction in their theta model to mimic the experimental results and found that a higher coefficient (0.94) was required for well-graded sands when compared to uniform sands (0.75). These differences were attributed to the presence of larger, heterogeneously distributed NAPL blobs in the graded sands. Because the dissolution experiments considered in this study were initiated at high NAPL saturations and large blobs were observed during these experiments [*Nambi and Powers*, 2000], the high coefficient on the NAPL saturation is consistent with the previous observations that this coefficient should increase with increasing heterogeneity in the blob size distribution.

5.2. Verification of the Model

[37] The correlation developed here (equation (6)) was used in conjunction with the transport equation to predict concentrations at the port immediately downgradient of the NAPL source zone for two independent experiments whose data was not used in the development of the correlation. A backward finite difference approximation scheme was employed to solve the one-dimensional transport equation in conjunction with a mass balance on the NAPL in the source zone. A time step of 30 min was employed to reduce the effects of numerical dispersion. The predictions were initiated for each of these experiments at a NAPL saturation of 0.35, the saturation below which mass transfer at the local scale was known to be the rate-limiting phenomenon [*Nambi and Powers*, 2000].

[38] The two independent experiments that were chosen for verification had widely varying initial NAPL saturations. Experiment 1 started with a high initial NAPL saturation (S_n = 0.73), although only data for $S_n < 0.35$ was used for the verification and experiment 2 started with a low initial NAPL saturation (S_n = 0.35). It can be seen from Figure 4 that the model incorporating equation (6) to describe NAPL dissolution rates is a reasonably good predictor of data from experiment 1 but a poor predictor of data from experiment 2. All the data used in the correlation (equation (6)) were from experiments that began with relatively high NAPL saturations (0.8–0.5). The initial NAPL saturation of experiment 1 falls within this range resulting in better predictions for that experiment. For experiment 2, the observed mass transfer was much more rapid than predicted by equation (6).

[39] Deviation between measured and predicted concentrations for experiment 2 that had a low initial saturation can be explained by analyzing the pore-scale distribution of NAPL in the different experiments. The distribution and shape of the NAPL blobs and, thus, the specific surface area that defines the mass transfer rate, depend upon the method of their formation. Multiphase flow phenomena and capillary forces can result in the entrapment of small NAPL blobs following the imbibition and drainage of a DNAPL. As shown in Figure 5b, discrete and uniformly distributed NAPL globules are generated in a homogeneous medium when capillary forces govern the entrapment process. The specific interfacial area in this case is large, resulting in relatively fast dissolution rates and rapid decreases in concentration with time. When the same NAPL saturation is attained by dissolution, pathways of preferential water flow cause bypassing of potentially large pockets of NAPL. The NAPL distribution in this case is not uniform and can be characterized as large and small blobs of different shapes separated by clean sand (Figure 5a). The extent of the development of the preferential pathways would depend on very small scale heterogeneities and the length of the NAPL source zone over which the pathways can develop. The large blobs that result from these preferential pathways have limited surface area and take a much longer time to dissolve. Thus, the time required to dissolve NAPL at

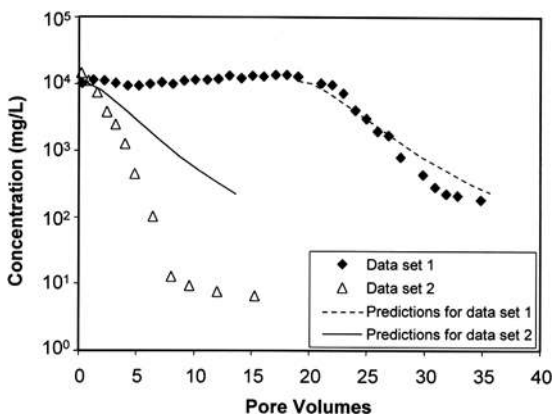

Figure 4. Comparison of experimental data and model predictions (equation (6)) for two independent data sets. Experiment 1 refers to an experiment that started with a high initial NAPL saturation (0.73) in the coarse lens. Experiment 2 refers to an experiment that started with a lower initial NAPL saturation (0.30) in the coarse lens.

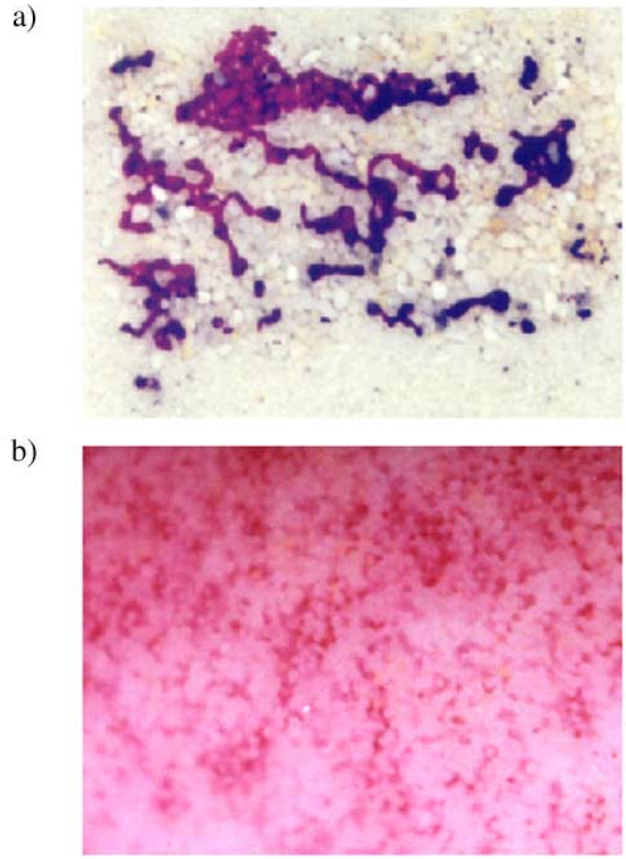

Figure 5. Photographs illustrating differences in NAPL distribution and blob shapes formed as result of different processes at similar NAPL saturations. (a) Residual saturation attained by NAPL dissolution from a source of high initial NAPL saturation. (b) Residual saturation attained by multiphase flow processes. Smaller, discrete, uniformly distributed NAPL blobs are formed in this second case.

equal saturations depends on the history of NAPL in the system. NAPL that was entrapped as discrete blobs by multiphase flow mechanism will dissolve faster than an equal saturation that was initially part of a NAPL pool with a high saturation.

[40] The NAPL distribution is further complicated by the relative rates of NAPL dissolution and NAPL redistribution. The NAPL considered in this research, o-toluidine, has a specific gravity very close to 1.0. Thus, there were minimal buoyancy forces acting on the NAPL to cause fluid flow during the experiment. For situations with a DNAPL with a higher density and lower solubility in highly permeable media (e.g., tetrachloroethene), the rate of NAPL migration might be faster than dissolution, resulting in a redistribution of the DNAPL as regions with preferential dissolution begin to develop.

[41] The significant impact that pore-scale regions of preferential flow can have on the overall dissolution process is similar to the concept of dissolution fingering defined by *Imhoff et al.* [1996]. They observed that preferential regions of dissolution occurred due to local variations in the effective permeability that affected the dissolution of NAPL originally entrapped at a residual saturation. The blob distribution illustrated in Figure 5a suggests that similar mechanisms affect the dissolution of NAPL initially present at a higher saturation as well.

[42] To further verify the speculation that the history of NAPL entrapment and dissolution has a significant impact on dissolution rates, the experimental results presented in Figure 4 were compared with the work of *Powers et al.* [1994]. Their mass transfer correlation was based on experimental data for dissolution from discrete styrene blobs generated by a series of multiphase displacements. The reduction in mass transfer rates resulting from the decrease in NAPL saturations over time was incorporated as a fraction of the initial residual saturation (θ_n/θ_n^o). This approach restricts the application of the *Powers et al.* [1994] model to systems with initial saturations on the order of 0.1 to 0.2. Thus rather than applying this model directly to the data from experiment 2, the original data from *Powers et al.* [1994] was reworked to eliminate the θ_n/θ_n^o term. Details of this data analysis are presented by *Nambi* [1999]. Results of the stepwise regression analysis of the reworked *Powers et al.* [1994] data set illustrated that the Reynolds number and NAPL saturation were the only two statistically significant parameters:

$$Sh' = 44.7 S_n^{0.937} \mathrm{Re}'^{0.526} \tag{7}$$

The R^2 value for this multiple regression was 0.945. Confidence intervals (95%) for each of the coefficients are $37.3 < \alpha < 53.7$; $0.905 < \beta_1 < 0.969$ and $0.438 < \beta_2 < 0.614$. Data used to develop this correlation include a wide range of saturations ($0.001 \leq S_n \leq 0.197$) and Reynolds numbers ($0.034 \leq Re' \leq 0.588$).

[43] Equation (7) was used to predict concentrations for experiment 2 to further assess the importance of the nature of the NAPL blob distribution on NAPL dissolution rates. Figure 6 illustrates that the rapidly decreasing concentrations observed in this experiment that began with a low saturation are well represented by the correlation that was

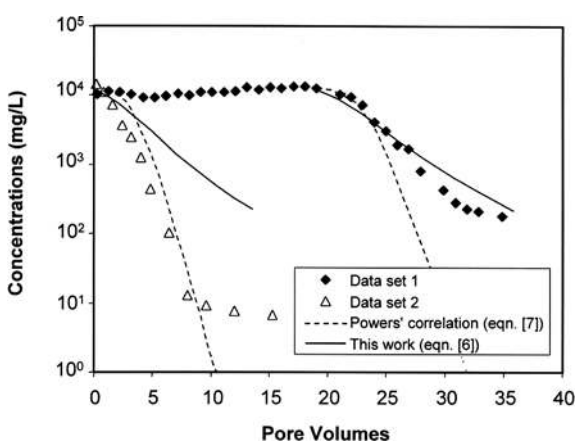

Figure 6. Comparison of predictions made using the new correlation developed here (equation (6)) to the correlation developed from data in homogeneous experimental cell (equation (7)) [*Powers et al.*, 1994]. Model predictions are presented for the same two independent experiments described in Figure 4.

Table 4. Results of Sensitivity Analysis

	Variations in Parameter Values	Correlations	R^2	Prediction Error[a]
Base case	Corey's equation for k_r; measured k_f	$37.2\ Re'^{0.61}\ S_n^{1.24}$	0.94	0.045
Case 1 (faster flow in coarse sand)	Wyllie's equation for k_r; measured k_f	$30.2\ Re'^{0.46}\ S_n^{1.27}$	0.95	0.027
Case 2 (faster flow in coarse sand)	Corey's equation for k_r; measured k_f were halved	$38.0\ Re'^{0.53}\ S_n^{1.27}$	0.94	0.023
Case 3 (slower flow in coarse sand)	Corey's equation for k_r; measured k_f were doubled	$34.7\ Re'^{0.65}\ S_n^{1.22}$	0.93	0.203
Case 4 (faster flow in coarse sand)	Wyllie's equation for k_r; measured k_f were halved	$32.4\ Re'^{0.40}\ S_n^{1.30}$	0.95	0.034

[a]Error = $\frac{1}{n}\sum_i (\log C_i^{pred} - \log C_i^{meas})^2$.

developed from experiments with a similar distribution of NAPL blobs. Predictions by equation (7), however, are not representative of concentrations from experiment 1 that started with high NAPL saturation. This experiment exhibited much slower dissolution rates than predicted by equation (7). This confirms our original hypothesis that correlations developed for homogeneous systems with low NAPL saturations (e.g., equation (7)) are inappropriate for heterogeneous systems with large range of NAPL saturations. Conversely, the correlation developed here (e.g., equation (6)) is appropriate for modeling the dissolution of NAPL that was initially present at a high saturation, but not for systems containing a residual saturation as obtained by multiphase flow processes. These results emphasize the inherent dependence of mass transfer rate coefficient correlations on the specific system they were developed for and suggest the need for very careful selection of a particular correlation based on similarity of mechanisms expected in the modeled system to those that were incorporated into the empirical correlation.

5.3. Sensitivity Analysis

[44] There is uncertainty in several of the parameters used in the development of equation (6). Error in the measured intrinsic permeability and uncertainty in the estimated relative permeability would affect the Reynolds number and therefore the estimated NAPL saturations: the two most critical parameters in the correlation. An analysis to assess the importance of these uncertainties was completed by varying these parameters in the analysis of the original data, recomputing the regression equations and comparing the results. The intrinsic permeability of the fine sand was increased to twice the measured value and later reduced to half the value in order to verify the impact of a possible positive or negative experimental error. The choice of relative permeability relationship between Corey's and Wyllie's equations was also considered. At high NAPL saturations, the Wyllie correlation ($k_r = S_e^3$ [*Wyllie*, 1962]) predicts relative permeabilities that are as much as an order of magnitude higher than the Corey equation. *Powers et al.* [1998] found this difference significant for their equilibrium modeling efforts. Three cases were considered in addition to the base case results presented above. Two cases had aqueous phase velocities that were higher than the base case; the third had slower velocities. Results of the regression analyses for each of these cases is presented in Table 4, with model predictions included in Figure 7. For all cases, the regression parameters (α, β_1, β_2) are within the 95% confidence intervals determined for the base case (equation (6)).

[45] Use of the Wyllie equation resulted in faster flow through the NAPL source zone (case 1). With this method for estimating the relative permeability, the mass transfer coefficient correlation improved modestly with a slight increase of $R^2 = 0.95$ as compared with $R^2 = 0.94$ in the base case. The increased flow rates through the coarse lens caused a decrease in the coefficient of Reynolds number (β_2), although the resulting values were within the 95% confidence interval for this coefficient. The case 1 model predictions showed a slight decrease in concentrations relative to the base case (Figure 7). The case 2 analysis, which also resulted in an increase in the aqueous phase velocity in the coarse sand, had a similar impact on the correlation as case 1 (Table 4 and Figure 7).

[46] From a comparison of the base case to case 1, it can be concluded that the model was not found to be sensitive to the choice of the relative permeability relationship. This conclusion differs from the conclusion drawn by *Powers et al.* [1998]. The reason for this discrepancy is that the model employed by *Powers et al.* [1998] was applied when the NAPL saturations were very high and hence the relative permeabilities were very low. At this stage, flow rates were very sensitive to changes in the NAPL saturation and relative permeabilities. Hence, any small variation in relative permeability estimates due to choice of the relationship used resulted in significant changes in predicted concentrations. At the lower NAPL saturations considered here ($S_n < 0.35$), the relative permeability is closer to unity and is significantly less influential in altering the flow rates.

[47] When the intrinsic permeability of the fine sands was doubled (case 3), the aqueous phase velocity in the NAPL source zone was predicted to be much slower and the coefficient of the Reynolds number was found to increase. A dramatic difference in the predicted concentrations was

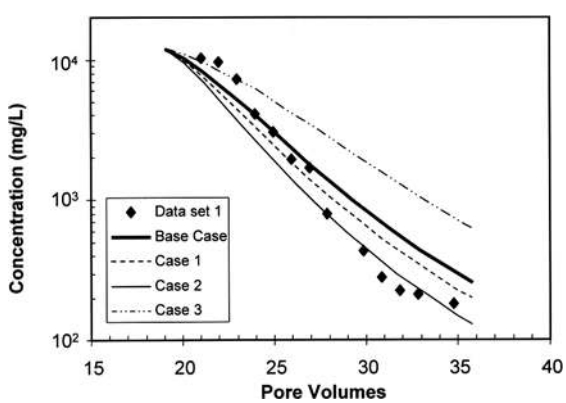

Figure 7. Illustration of the sensitivity of the model to uncertainty in relative permeability relationship and/or intrinsic permeability values. Table 2 describes parameters used for the four separate simulations.

observed, with a longer tailing period predicted. Thus we can conclude that the correlation is sensitive to the value of intrinsic permeability of the sands within a reasonable range of accuracy. It is thus very important to obtain accurate measurements of intrinsic permeability in order to obtain good predictions from the model.

[48] In contrast, the exponent values for the saturation term did not vary significantly regardless of the parameters considered in the sensitivity analysis (Table 4). This suggests that the conclusions reached above regarding the impact of blob distribution on this exponent are legitimate: higher exponent values are required for larger more amorphous blob distributions.

6. Summary and Conclusions

[49] A new correlation was developed for predicting rate limited mass transfer within a NAPL source zone entrapped in heterogeneous systems. The correlation was based on data from experiments in two-dimensional heterogeneous systems with high initial NAPL saturations. For saturations $>\sim 0.35$, a local equilibrium assumption can be used to estimate the mass transfer rates. As the NAPL saturation continues to drop due to dissolution, the new mass transfer correlation, (equation (6)) should be used. This correlation was developed from data with a wide rage of saturations ($0.0001 < S_n < 0.35$) and Reynolds numbers ($0.018 < \mathrm{Re}' < 0.134$). Only two independent variables, NAPL saturation and Reynolds number were critical parameters influencing mass transfer for the experimental conditions considered. All the other independent variables that were considered were found to be statistically insignificant. The coefficient on the Reynolds number was within the range of the existing mass transfer correlations whereas the coefficient on the NAPL saturation was higher than those found by others. The incorporation of relatively high NAPL saturations that included larger blobs with complex shapes contributed to the higher coefficient on the NAPL saturation.

[50] The correlation developed here was incorporated in a finite difference model for solute transport to predict concentrations from two independent experiments that began at widely varying initial NAPL saturations. The model was able to adequately predict concentrations from the experiment with an initially high NAPL saturation. Concentrations were over predicted, however, for an experiment with a lower initial NAPL saturation. Distinct differences in the NAPL blob distribution between these two experiments at similar NAPL saturations can explain variability in the dissolution histories. NAPL blobs entrapped via immiscible displacement processes tend to be smaller, discrete globules, while those developed following the dissolution of an initially high saturation of NAPL tend to be much larger due to dissolution fingering. Very different mass transfer coefficient correlations are required depending on this history. Hence, a considerable amount of discretion is required in applying the appropriate correlations in order to predict NAPL dissolution in heterogeneous systems. To aid in the judgment process, a sound knowledge of the multiphase flow and dissolution history that generated a given NAPL saturation distribution is also necessary. As with any mass transfer correlation, error should be expected when mass transfer correlations are extrapolated for application to systems other than which they were developed.

[51] **Acknowledgments.** Funding for this research was provided by the National Science Foundation under grant BCS-9308131. Any opinions, findings, conclusions or recommendations expressed in this manuscript are those of the authors and do not necessarily reflect the views of the National Science Foundation.

References

Abriola, L. M., Modeling multiphase migration of organic chemicals in ground water systems—A review and assessment, *Environ. Health Perspect.*, *83*, 117–143, 1989.

American Society for Testing and Materials (ASTM), ASTM D2434-68 (2000) Standard test method for permeability of granular soils (constant head), West Conshohocken, Pa., 1993. (Available at http://enterprise.astm.org/PAGES/D2434.htm).

Berglund, S., Aquifer remediation by pumping: A model for stochastic-advective transport with nonaqueous phase liquid dissolution, *Water Resour. Res.*, *33*(4), 649–661, 1997.

Brusseau, M. L., Z. Zhang, N. T. Nelson, R. B. Cain, G. R. Tick, and M. Oostrom, Dissolution of nonuniformly distributed immiscible liquid: Intermediate-scale experiments and mathematical modeling, *Environ. Sci. Technol.*, *36*(5), 1033–1041, 2002.

Chatzis, I., N. R. Morrow, and H. T. Lim, Magnitude and detailed structure of residual oil saturation, *SPEJ Soc. Pet. Eng. J.*, *23*, 311–326, 1983.

Chrysikopoulos, C. V., and T. J. Kim, Local mass transfer correlations for nonaqueous phase liquid pool dissolution in saturated porous media, *Transp. Porous Media*, *38*(1–2), 167–187, 2000.

Conrad, S. H., J. L. Wilson, W. R. Mason, and W. J. Peplinski, Visualization of residual organic liquid trapped in aquifers, *Water Resour. Res.*, *28*(2), 467–478, 1992.

Corey, A. T., The interrelation between gas and oil relative permeabilities, *Prod. Mon.*, *19*(1), 38–41, 1954.

Cussler, E. L., *Diffusion: Mass Transfer in Fluid Systems*, 2nd ed., Cambridge Univ. Press, New York, 1997.

Dekker, T. J., and L. M. Abriola, The influence of field-scale heterogeneity on the infiltration and entrapment of dense nonaqueous phase liquids in saturated formations, *J. Contam. Hydrol.*, *42*(2–4), 187–218, 2000.

Dillard, L. A., and M. J. Blunt, Development of a pore network simulation model to study nonaqueous phase liquid dissolution, *Water Resour. Res.*, *36*(2), 439–454, 2000.

Frind, E. O., J. W. Molsen, and M. Schirmer, Dissolution and mass transfer of multiple organics under field conditions: The Borden emplaced source, *Water Resour. Res.*, *35*(3), 683–694, 1999.

Geller, J. T., and J. R. Hunt, Mass transfer from nonaqueous phase organic liquids in water-saturated porous media, *Water Resour. Res.*, *29*(4), 833–845, 1993.

Hunt, J. R., N. Sitar, and K. S. Udell, Non-aqueous phase liquid transport and cleanup, 1, Analysis of mechanism, *Water Resour. Res.*, *24*(8), 1247–1258, 1988.

Illangasekare, T. H., E. J. Armbruster III, and D. N. Yates, Nonaqueous phase fluids in heterogeneous aquifers—Experimental study, *J. Environ. Eng.*, *121*(8), 571–579, 1995.

Imhoff, P. T., M. H. Arthur, and C. T. Miller, An experimental study of complete dissolution of a nonaqueous phase liquid in saturated porous media, *Water Resour. Res.*, *30*(2), 307–320, 1994.

Imhoff, P. T., G. P. Thyrum, and C. T. Miller, Dissolution fingering during solubilization of nonaqueous phase liquids in saturated porous media, 2, Experimental observations, *Water Resour. Res.*, *32*(7), 1929–1942, 1996.

Jia, C., K. Shing, and Y. C. Yortos, Visualization and simulation of non-aqueous phase liquids solubilization in pore networks, *J. Contam. Hydrol.*, *35*(4), 363–387, 1999.

Kim, T. J., and C. V. Chrysikopoulos, Mass transfer correlations for non-aqueous phase liquid pool dissolution in saturated porous media, *Water Resour. Res.*, *35*(2), 449–459, 1999.

Knutson, C. E., C. J. Werth, and A. J. Valocchi, Pore-scale modeling of dissolution from variably distributed nonaqueous phase liquid blobs, *Water Resour. Res.*, *37*(12), 2951–2963, 2001.

Kueper, B. H., W. Abbot, and G. Farquhar, Experimental observations of multiphase flow in heterogeneous porous media, *J. Contam. Hydrol.*, *5*(1), 83–95, 1989.

Kueper, B. H., D. Redman, R. C. Starr, S. Reitsma, and M. Mah, A field experiment to study the behavior of tetrachloroethylene below the water

table: Spatial distribution of DNAPL residual and pooled NAPL, *Ground Water*, *31*(5), 756–766, 1993.

Lamarche, P., Dissolution of immiscible organics in porous media, Ph.D. dissertation. Univ. of Waterloo, Waterloo, Ontario, Canada, 1991.

Mayer, A. S., and C. T. Miller, The influence of mass transfer characteristics and porous media heterogeneity on nonaqueous phase dissolution, *Water Resour. Res.*, *32*(6), 1551–1568, 1996.

Mendenhall, W., and T. Sincich, *Statistics for Engineering and the Sciences*, 4th ed., Prentice-Hall, Old Tappan, N. J., 1994.

Miller, C. T., M. M. Poirer-McNeill, and A. S. Mayer, Dissolution of trapped nonaqueous phase liquids: Mass transfer characteristics, *Water Resour. Res.*, *26*(11), 2783–2796, 1990.

Nambi, I. M., Dissolution of non-aqueous phase liquids in heterogeneous subsurface systems, Ph.D. dissertation, Dep. of Civ. and Environ. Eng., Clarkson Univ., Potsdam, N. Y., 1999.

Nambi, I. M., and S. E. Powers, NAPL dissolution in heterogeneous systems: An experimental Study in a simplified heterogeneous system, *J. Contam. Hydrol.*, *44*(2), 161–184, 2000.

Powers, S. E., C. O. Loureiro, L. M. Abriola, and W. J. Weber Jr., Theoretical study of the significance of nonequilibrium dissolution of nonaqueous phase liquids in subsurface systems, *Water Resour. Res.*, *27*(4), 463–478, 1991.

Powers, S. E., L. M. Abriola, and W. J. Weber Jr., An experimental investigation of NAPL dissolution in saturated subsurface systems: Steady-state mass transfer rates, *Water Resour. Res.*, *28*(10), 2691–2706, 1992.

Powers, S. E., L. M. Abriola, and W. J. Weber Jr., An experimental investigation of NAPL dissolution in saturated subsurface systems: Transient mass transfer rates, *Water Resour. Res.*, *30*(2), 321–332, 1994.

Powers, S. E., I. M. Nambi, and G. W. Curry Jr., NAPL dissolution in heterogeneous systems: Mechanisms and a local equilibrium modeling approach, *Water Resour. Res.*, *34*(12), 3293–3302, 1998.

Saba, T., and T. H. Illangasekare, Effect of groundwater flow dimensionality on mass transfer from entrapped nonaqueous phase liquid contaminants, *Water Resour. Res.*, *36*(4), 971–980, 2000.

Soerens, S. T., D. A. Sabatini, and J. H. Harwell, Effects of flow bypassing and nonuniform NAPL distribution on the mass transfer characteristics of NAPL dissolution, *Water Resour. Res.*, *34*(7), 1657–1673, 1998.

Treybal, R. E., *Mass Transfer Operations*, 3rd ed., McGraw-Hill, New York, 1980.

Unger, A. J. A., P. A. Forsyth, and E. A. Sudicky, Influence of alternative dissolution models and subsurface heterogeneity on DNAPL disappearance times, *J. Contam. Hydrol.*, *30*, 217–242, 1998.

Wilson, J. L., S. H. Conrad, W. R. Mason, W. Peplinski, and E. Hagan, Laboratory investigations of residual organic liquids from spills, leaks, and disposal of hazardous wastes in groundwater, *EPA/600/6-90/004*, U. S. Environ. Prot. Agency, Washington, D. C., 1990.

Wyllie, M. R. J., Relative Permeability, in *Petroleum Production Handbook*, vol. II, *Reservoir Engineering*, edited by T. C. Taylor and R. W. Frick, pp. 25.1–25.14, McGraw-Hill, New York, 1962.

Zhou, D. G., L. A. Dillard, and M. J. Blunt, A physically based model of dissolution of nonaqueous phase liquids in the saturated zone, *Transp. Porous Media*, *39*(2), 227–255, 2000.

Zhu, J., and J. F. Sykes, The influence of NAPL dissolution characteristics on field-scale contaminant transport in the subsurface, *J. Contam. Hydrol.*, *41*, 133–154, 2000.

I. M. Nambi, Department of Civil and Environmental Engineering, 4142 Newmark Civil Engineering Laboratories, University of Illinois, Urbana, IL 61801, USA. (nambi@uiuc.edu)

S. E. Powers, Department of Civil and Environmental Engineering, Clarkson University, Potsdam, NY 13699-5710, USA. (sep@clarkson.edu)